

Dynamic fracture mechanics of a RIM polyamide block copolymer reinforced with glass strand mat*

J. Karger-Kocsis**

Institute for Composite Materials, University of Kaiserslautern, D-6750 Kaiserslautern, Federal Republic of Germany

ABSTRACT

The fracture behavior of a reaction injection molded (RIM) polyamide block copolymer reinforced with randomly arranged continuous glass fiber bundles (glass mats) was studied under dynamic loading conditions at $T=RT$ and $T=-40$ °C. Dynamic fracture toughness, K_{Ic} , and fracture energy, G_{Ic} , values were derived from instrumented high-speed impact bending tests carried out on Charpy and Izod specimens of different size and notching direction, respectively. It was established that fracture mechanics data depend on the ligament width of the specimens. It was shown how the "inherent" flaws caused by machining and molding can be determined. Failure mode of the composites was characterized by fractography and possible failure events were summarized. Recommendations were given for further material improvements.

INTRODUCTION

Reinforced reaction injection molded polyamide block copolymers reinforced with continuous swirl glass fiber mat (PA-RRIM) are promising candidates to replace metals in the automobile industry. This target application requires a profound fracture mechanical characterization of the PA-RRIM composites. The aim of this contribution is to give informations about dynamic fracture mechanical data from high-speed impact measurements carried out at different testing conditions as well as to clarify the related failure behavior.

EXPERIMENTAL

Materials

The plates investigated ($150 \times 150 \times 4$ mm³) were molded by RAPRA Technology Ltd (Shawbury, GB) using the components of the Nyrim^R 2000 system of DSM (Maastricht, NL). This PA-RIM material was a block copolymer containing 20 wt.% elastomeric polyether soft segments.

Fiber loading ($\approx 20-50$ wt.%) were produced by stacking continuous E-glass strand mats (Unifilo U816 swirl mat from Vetrotex International, Aix-les-Bains, F) into the mold prior RIM. This GF mat of 450 g/m² surface weight was sized by a silane derivative and bonded by a polyester binder. The strands with a diameter of

*Work presented at the ECCM-4 Conference (25.-28. Sept. 1990) in Stuttgart, FRG

**Present and mailing address: Polymer and Composites Group, TU Hamburg-Harburg, P.O. Box 901403, D-2100 Hamburg 90, FRG

about 150 μm were composed from GF monofilaments of 15 μm diameter and 25 tex strength.

Methods

For the dynamic fracture characterization instrumented high-speed impact bending techniques were used. Charpy specimens of different size and notching were cut from the plaques according to Figure 1 and impacted at $v=3.7$ m/s striker speed (DIN 53 455 standard). The dynamic fracture characterization was extended to Izod specimens (cf. Figure 1) too, fractured at $v=3.46$ m/s (ASTM D 256 standard). Measurements were followed in both cases at different temperatures ($T=-40$ and 20 $^{\circ}\text{C}$) using an instrumented impact pendulum device. This device was connected to an AFS-MK3 fractoscope (Ceast, Torino, I) and additionally to a Hewlett-Packard computer for data acquisition and storage by means of a home-made program.

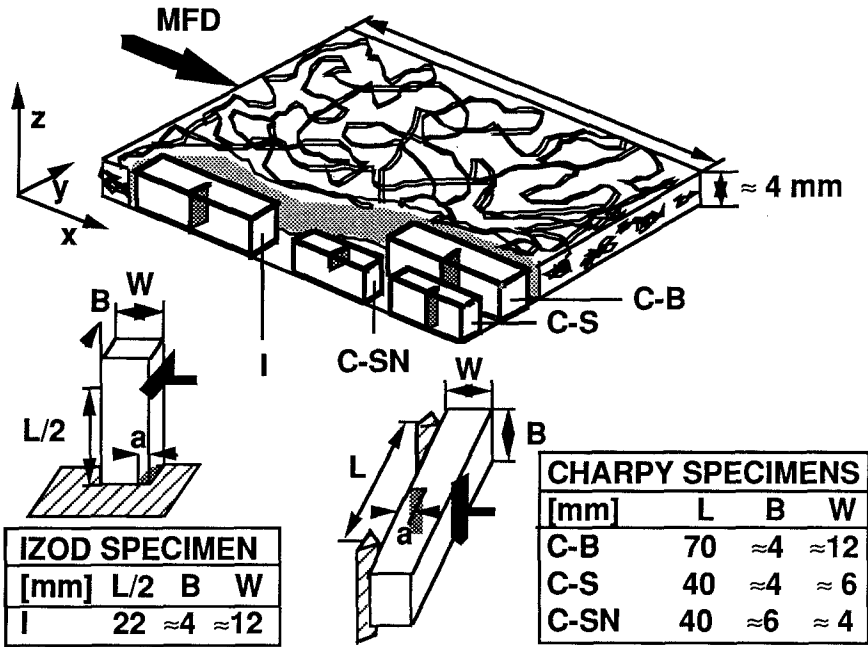


Figure 1. Machining, notching, dimension and impact mode of the specimens used

From the data registered and evaluated both the dynamic stress intensity factor or fracture toughness, K_d , and the dynamic strain energy release rate or fracture energy, G_d , were determined. K_d was got as the slope of a straight line through the origo giving the best fit for the $\sigma \cdot Y$ vs. $a^{-1/2}$ point pairs, where " σ " is the maximum stress, " Y " is the shape factor and " a " is the notch length. Since the shape factor of the Izod specimens is unknown a related value from the Charpy range has been used.

G_d was determined as the slope of a straight line running through the origo by plotting the E vs. $BW\phi$ values, where " E " is the energy absorbed, " B " and " W " are the specimen thickness and width, respectively (cf. Figure 1), and " ϕ " is the energy calibration factor. Detailed informations about the evaluation methods used can be taken from the literature (e.g. [1-3]). By the selection of the specimens to be impacted and differing from each other in type, size and razor blade notching answers for the following questions were expected:

- i- which is the effect of specimen size on fracture mechanical data (cutting results from the initial continuous fiber reinforced composite a "chopped" fiber reinforced version)
- ii- is there any anisotropy in the mechanical response of the matrix and of the preplaced GF mat reinforced composites
- iii- whether machining (sawing) additional flaws originates

RESULTS AND DISCUSSION

Effect of Specimen Size and Notching Matrix

Figure 2 shows the K_d and $G_{d,i}$ evaluation for the matrix at different specimens. $G_{d,i}$ denotes the initial fracture energy, representing either the onset of catastrophic fracture at the maximum stress for brittle or the onset of crack propagation for ductile failure, respectively. This term was used since complete separation of the specimen not always occurred. The K_d values of the matrix were found in the range of 2.8 to 3.6 $\text{MPa}\sqrt{\text{m}}$ for the different specimens, i.e. within a reasonable scatter (Figure 2a). The $G_{d,i}$ values got on different specimens agreed again very well with each other (from 9.2 to 11.2 kJ/m^2 ; cf. Figure 2b) with the only exception of the related value for the C-SN specimens ($\approx 5 \text{ kJ/m}^2$). This can be explained by the molding-induced skin-core morphology, which showed flow line contours according to light microscopic pictures. Analogous morphology was reported for linear polyesters [4] and polyamides [5].

Composites

Both the K_d and $G_{d,i}$ values of the PA-RRIM composites increased according to the following sequence:

$$\text{C-SN} \approx \text{C-S} < \text{I} < \text{C-B.}$$

This trend suggests that there is an effect of ligament width and thus of specimen size related with an effective network size of the GF strand mat. Since the width of the Izod (I) and big Charpy (C-B) specimens was the same (cf. Figure 1) one expected similar values. In spite of this a slight but reproducible difference was found according to the above ranking. It may be connected with the difference in the clamping of the specimens and thus with the related stress state upon bending. Since the fracture mechanics data were practically the same for the small Charpy specimens (C-S, C-SN) the GF mat applied can be treated as an isotropic reinforcement.

The evaluation method of $G_{d,i}$ allowed an estimation of the flaw size induced by machining (Figure 3). In this case the "ineffective" notch size (causing fracture away from the notch introduced by a razor blade) agreed exactly with the value

derived by the method proposed by Akay and Barkley [6]. This machining induced flaw size proved to be in the range of 0.6 to 1.2 mm depending on the test conditions, specimen size and type.

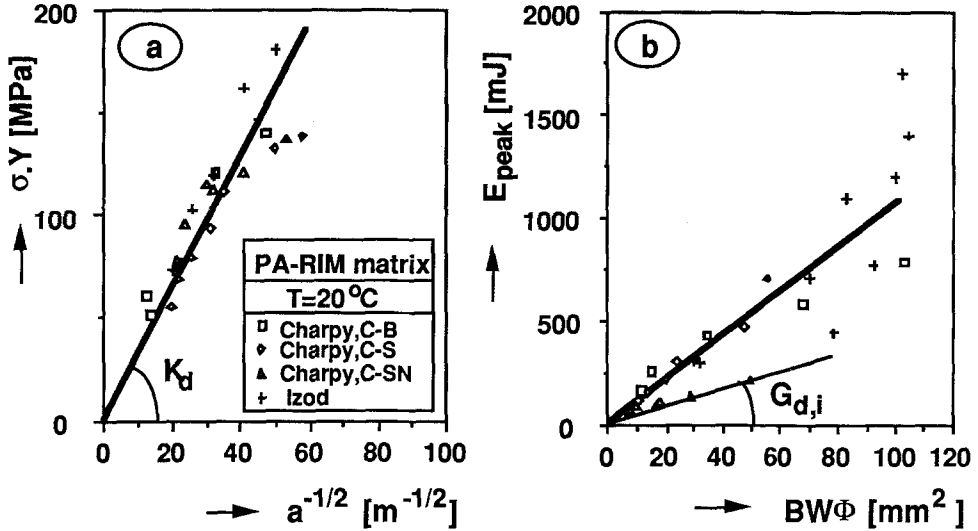


Figure 2. Evaluation of K_d (a) and $G_{d,i}$ (b) on different specimens for the PA-RIM matrix

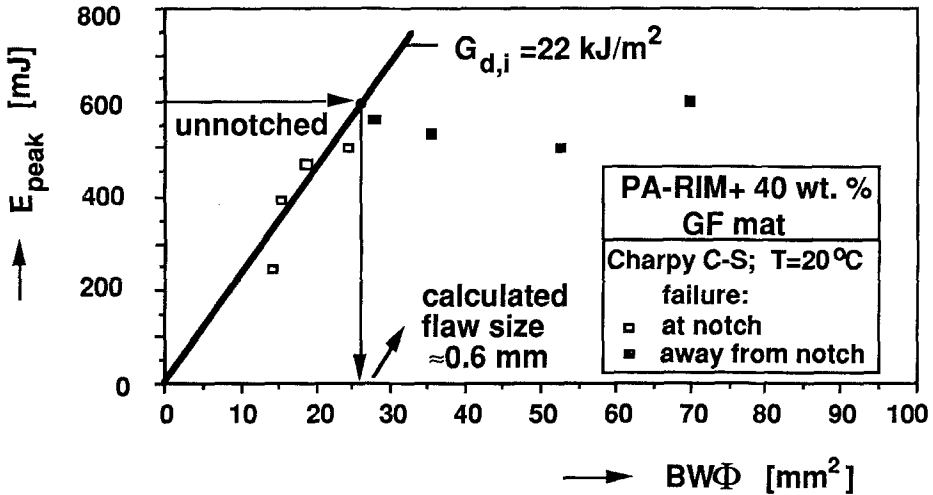


Figure 3. Evaluation of $G_{d,i}$ and determination of the sawing-induced flaw size of a PA-RRIM with 40 wt.% GF mat

About the molding-induced "inherent" flaw size tests performed on C-SN specimens (cf. Figures 1 and 6b) delivered informations. Its size was found between 0.2 and 0.4 mm.

Effect of Fiber Loading

The effect of GF mat loading on K_d and $G_{d,i}$ is demonstrated in Figure 4. According to this Figure both K_d and $G_{d,i}$ increase with V_f , the increment is, however, less steep at higher V_f . These $G_{d,i}$ values are smaller than the related ones published by Otaigbe and Harland [7] for a GF mat reinforced PA-6. This difference can be explained by a matrix effect, since PA-6 used in the cited work is more stiff than our "inherently plastified" polyamide block copolymer (in the literature often called as nylon block copolymer, NBC).

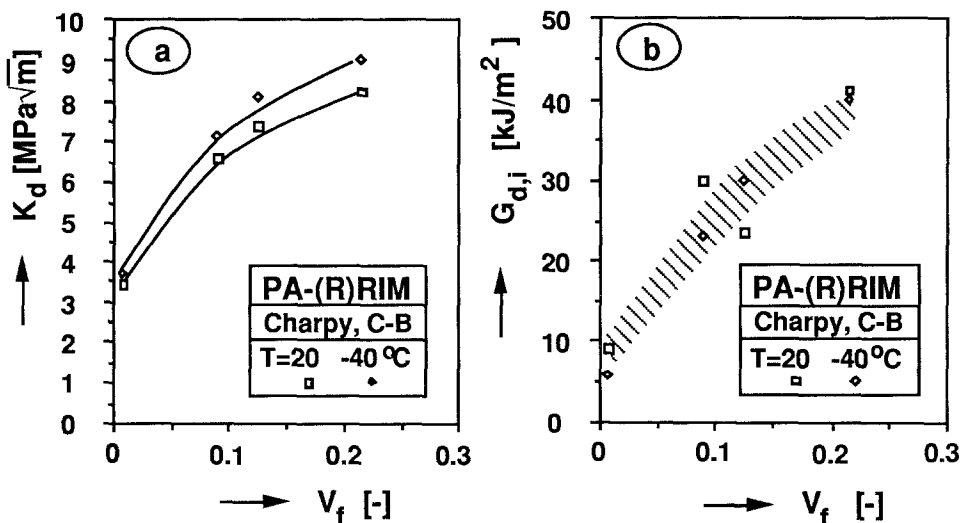


Figure 4.

Effect of temperature (T) on the K_d (a) and $G_{d,i}$ values (b) of the PA-RRIM composites with GF strand mat

Effect of Temperature

Based on the results in Figure 4 the effect of temperature is negligible in the temperature range studied. This statement relates especially for the PA-RRIM composites.

Failure Behavior

Matrix

The PA-RIM matrix fails (micro)ductilely depending upon the testing temperature in this case. On the fracture surface characteristic markings of secondary cracking could be resolved. It was proved by energy dispersive X-ray scattering (EDAX) that their initiation sites are not dissolved catalyst rests [8].

Composites

The incorporation of swirl GF mat alters the failure manner basically. Among the fiber-related failure events fiber bridging due to a "mesh deformation" of the mat in the ductile matrix

becomes very important, this process is namely responsible why complete separation of the specimens is very seldom (Figure 5).

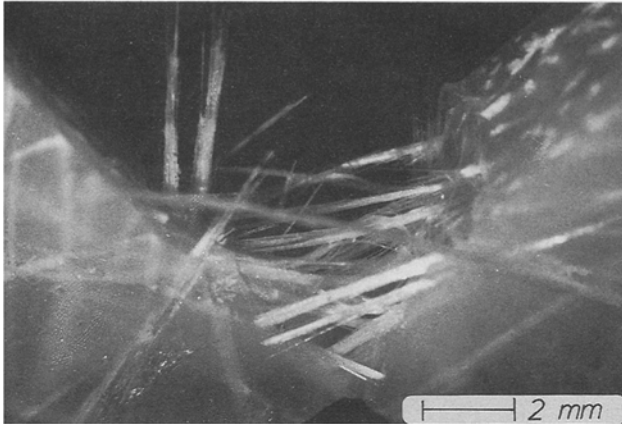


Figure 5.

Macrophotograph taken from an impacted C-B specimen of PA-RRIM with 20 wt.% GF strand mat (Notching from the top)

Among other peculiarities of PA-RRIM the intraroving breakage and fibrillization of the strands after local pull-out processes should be mentioned (Figure 6). These events contribute to the energy dissipation in the damage zone, the exact size of which can hardly be determined.

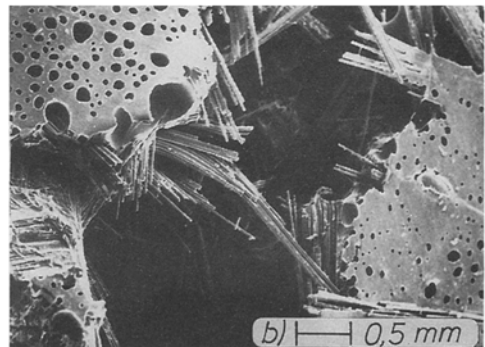
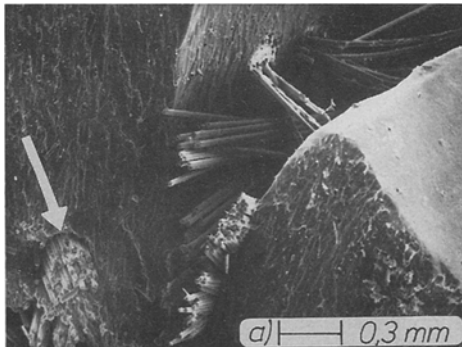


Figure 6.

SEM pictures on the C-SN specimens of the PA-RRIM with 20 (a) and 50 wt. % GF strand mat (b), respectively

- a) notching from the top, notch depth 0.5 mm, arrow indicates a strand cut by sawing which may act as a flaw when tested in form of a C-S specimen
- b) specimen without notch, the surface topology is caused by air bubbles the size of which is connected with the molding-induced or "inherent" flaw.

It is worth mentioning that all PA-RRIM composites exhibited a stable fracture propagation stage, their final failure never occurred by catastrophic manner. It was reported in the literature [7] that the energy values in the fracture initiation

(ended up by Epeak used in Gd_i evaluation) and fracture propagation range related to each other may be used as an indicator of brittle or ductile failure behavior. Due to incomplete separation of the specimens the energy absorbed during crack propagation could hardly be estimated in our case.

Recommendations for Material Improvement

The presence of catalyst rests is rather characteristic for all PA-RIM matrices. Since they act as stress concentrators and induce undesired secondary cracks the dissolution of the catalyst should be improved. It is also suggested to increase the "network mesh deformability" of the GF mat by a proper "structuring" of the mat. Use of coupling and sizing agents - provided that the polymerization is unaffected - seems to be also beneficial as it is the case in all polyamide matrix systems [9].

From the point of view of molding the main problem is associated with the escape of the air during wetting of the prelocated GF mat by the molten RIM system. Adequate tool and processing modifications might reduce the surface flaws (cf. Figure 6b), caused by the air compressed, considerably.

CONCLUSIONS

Improved fracture mechanical data can be noticed for the PA-RRIM composites with GF mat reinforcement when one compares the corresponding values of chopped and mat reinforced composites [8-9]. The upgrading is more obvious at high-frequency (based on the fracture time in the fractograms the frequency of the impact bending tests was in the range of 10^2 - 10^3 Hz) than at low frequency loadings (e.g. static fracture or creep measurements), so thus PA-RRIM with GF mat reinforcement is a material of outstanding impact resistance.

ACKNOWLEDGEMENT

The financial support of this study by the EURAM program of the European Community (MA 1E/0043/C) is gratefully acknowledged.

REFERENCES

- 1 Williams, J.G.: Fracture Mechanics of Polymers, Ellis Horwood Ltd., Chichester, 1984
- 2 Savadori, A.: Polym. Test., 5 (1985), 209
- 3 Plati, E. and Williams, J.G.: Polym. Eng. Sci., 15 (1975), 470
- 4 Callear, J.E. and Shortall, J.B.: J. Mater. Sci., 12 (1977), 141
- 5 Karger-Kocsis, J. and Friedrich, K.: Plast. Rubb. Process. Appl., 12 (1989), 63
- 6 Akay, M. and Barkley, D.: Polym. Test., 7 (1987), 391
- 7 Otaigbe, J.U. and Harland, W.G.: J. Appl. Polym. Sci., 37 (1989) 77

- 8 Karger-Kocsis, J.: Structure and fracture mechanics of injection molded composites in "Encyclopedia of Composites" (Ed.: Lee, S.M.), VCH Publ., N.Y., (to be appeared)
- 9 Friedrich, K. and Karger-Kocsis, J.: Fracture and fatigue of unfilled and reinforced polyamides and polyesters in "Solid State Behavior of Linear Polyesters and Polyamides" (Eds.: Schultz, J.M and Fakirov, S.), Prentice Hall Inc., Englewood Cliff, 1990, p.248

Accepted June 15, 1990

C